Journal of Systems Engineering and Electronics
Vol. 32, No. 6, December 2021, pp.1463 – 1476

Self-organized search-attack mission planning for UAV swarm based on wolf pack hunting behavior

HU Jinqiang[1], WU Husheng[1,*], ZHAN Renjun[1], MENASSEL Rafik[2], and ZHOU Xuanwu[3]

1. School of Equipment Management and Support, Armed Police Force Engineering University, Xi'an 710086, China;
2. Department of Mathematics and Computer Science, Tebessa University, Tebessa 12002, Algeria;
3. Foundation Department, Armed Police Command College, Tianjin 300250, China

Abstract: Cooperative search-attack is an important application of unmanned aerial vehicle (UAV) swarm in military field. The coupling between path planning and task allocation, the heterogeneity of UAVs, and the dynamic nature of task environment greatly increase the complexity and difficulty of the UAV swarm cooperative search-attack mission planning problem. Inspired by the collaborative hunting behavior of wolf pack, a distributed self-organizing method for UAV swarm search-attack mission planning is proposed. First, to solve the multi-target search problem in unknown environments, a wolf scouting behavior-inspired cooperative search algorithm for UAV swarm is designed. Second, a distributed self-organizing task allocation algorithm for UAV swarm cooperative attacking of targets is proposed by analyzing the flexible labor division behavior of wolves. By abstracting the UAV as a simple artificial wolf agent, the flexible motion planning and group task coordinating for UAV swarm can be realized by self-organizing. The effectiveness of the proposed method is verified by a set of simulation experiments, the stability and scalability are evaluated, and the integrated solution for the coupled path planning and task allocation problems for the UAV swarm cooperative search-attack task can be well performed.

Keywords: search-attack mission planning, unmanned aerial vehicle (UAV) swarm, wolf pack, hunting behavior, swarm intelligence, labor division.

DOI: 10.23919/JSEE.2021.000124

1. Introduction

The unmanned aerial vehicle (UAV) has been widely used to perform dull, dangerous, and dirty (3D) tasks in civil and military fields. Due to the capability limitation of a single UAV in complex mission environment, UAV swarm has attracted increasing attention because of its higher working efficiency, stronger task capability, and better system robustness [1,2]. In the military field, cooperative search-attack in unknown environments is an important application of UAV swarms, and the efficient mission planning technology is the basis for UAV swarms to perform the cooperative search-attack task autonomously [3,4]. Due to the complex and dynamic nature of task environments, the tight coupling between UAV path planning and task allocation, and the heterogeneity of UAVs, UAV swarm cooperative mission planning (USCMP) has become a challenging problem.

Many scholars use the layered decoupling method to decompose USCMP into two separate issues of task allocation and path planning [5,6]. In this way, the solution difficulty of USCMP can be reduced and the calculation speed can be improved efficiently [7]. However, the task allocation scheme has weak practicability. Considering the coupling between task allocation and path planning, it is feasible to adopt the integrated solving methods for USCMP [8,9]. By taking the path length of UAVs as a variable of the task allocation cost function, the flight paths meeting the restrictions on mobility of UAVs and the task allocation scheme can be generated simultaneously [10]. The centralized integrated algorithms can decouple task allocation and path planning preferably [11−13], while the calculation is completely conducted on the ground station or a single UAV which acts as the central node due to the centralized architecture, and the centralized integrated algorithms have the defects of high computational cost, strong dependence of communication link, and easily getting into single-point failure.

By comparison, the distributed integrated algorithms show the advantages of high system reliability and scalability [14,15]. Recently, diverse algorithms for USCMP based on the distributed architecture have been

Manuscript received November 29, 2020.
*Corresponding author.
This work was supported by the National Natural Science Foundation of China (61502534), the Shaanxi Provincial Natural Science Foundation (2020JQ-493), the Integrative Equipment Research Project of Armed Police Force (WJ20211A030018), the Military Science Project of the National Social Science Fund (WJ2019-SKJJ-C-092), and the Theoretical Research Foundation of Armed Police Engineering University (WJY202148).

proposed, such as the contract network-based algorithm (CNBA) [16], the distributed ant colony optimization (DACO) [17], the distributed genetic algorithm (DGA) [18] and the consensus-based bundle algorithm (CBBA) [19]. Though the aforementioned algorithms can obtain the optimal solution for a specific task scenario, their real-time performance and dynamic response capability are not ideal because the mission planning problem needs to be reconstructed when the mission environment changes.

In nature, some social organisms (e.g., ant colony, bee colony, and wolf pack) are highly similar to UAV swarm in terms of the distribution of organizational structure, the simplicity of individuals, the flexibility of action mode and the emergence of swarm intelligence (SI) [20]. Therefore, some scholars tried to design novel distributed integrated algorithms for USCMP by simulating the complex and orderly collective behaviors of social organisms. Kim et al. [21] established an integrated model of UAV swarm cooperative search-attack task allocation, and solved it by using the response-threshold model (RTM). RTM simulates the labor division behavior of ant colony, and each ant agent can make a probabilistic decision on the task execution autonomously according to the task stimulus and individual response threshold. Wu et al. [22] proposed a dynamic ant colony labor division (DACLD) model to solve the UAV swarm combat task allocation problem by designing the dynamic task stimulus and response threshold. Kurdi et al. designed the bacterial foraging behavior-based [23] and the locust elastic behavior-based [24] multi-UAV task allocation methods for pest management and disaster rescue, respectively. The basic mechanism of these methods is that each UAV is abstracted and modeled as a simple individual of biological groups. Based on the local perception and interaction rule, corresponding optimization and coordination strategies for individuals to dynamically respond to the external and internal changes are designed, so as to realize the self-organized and flexible motion planning and group task coordinating for UAV swarm. In essence, by following the bottom-to-up solving idea and simulating individuals' behavioral mechanism of dynamic response to the environment, these algorithms have outstanding advantages of simple calculation, high degree of self-organization, and environmental adaptability.

Wolves are social animals with high intelligence [25]. The cooperative hunting behavior of wolf pack shows clear division of labor, efficient collaboration, strict organization, and behavioral flexibility [26,27]. Based on the wolf pack's cooperative hunting behavior, this study proposes a distributed self-organizing search-attack mission planning method for UAV swarm. The main contributions of this study are as follows: First, to solve the multi-target search problem in unknown environments, a wolf scouting behavior-inspired cooperative covering search algorithm for UAV swarm is designed. Second, a distributed self-organizing task allocation algorithm for UAV swarm cooperatively attacking targets is proposed by analyzing the flexible labor division behavior of wolves. Considering the target value, target resource requirement, path cost, and available resources, the artificial wolf agents can adjust their specific roles and allocate the subtasks flexibly based on the simple rules of local interaction and perception, so as to complete integrated solution for path planning and task allocation of the UAV swarm.

The remainder of this paper is arranged as follows: Section 2 describes the UAV swarm cooperative search-attack mission planning problem. Section 3 designs a wolf scouting behavior-inspired cooperative search algorithm. Section 4 proposes a distributed self-organizing task allocation algorithm based on wolf pack labor division behavior. In Section 5, the performances of the proposed search algorithm and the task allocation algorithm are evaluated by a set of simulation experiments, and this study is concluded in Section 6.

2. Description of UAV swarm cooperative search-attack mission planning problem

There is a heterogeneous UAV swarm composed of N_1 reconnaissance UAVs (R-UAVs) $U^A=\left\{U_1^A,U_2^A,\cdots,U_{N_1}^A\right\}$ and N_2 integrated reconnaissance/strike UAVs (RS-UAVs) $U^B=\left\{U_1^B,U_2^B,\cdots,U_{N_2}^B\right\}$ in the battlefield, which aims to search and attack multiple unknown targets. The heterogeneity of UAVs is mainly reflected in their payloads. Both R-UAVs and RS-UAVs can carry the non-consumptive reconnaissance resources such as laser irradiation and infrared detection equipment, while RS-UAVs can carry consumptive resources of attack ammunition. The n types of consumptive resources of the ith RS-UAV U_i are denoted by

$$\boldsymbol{R}^{U_i}=(R_1^{U_i},R_2^{U_i},\cdots,R_n^{U_i}),\quad i=1,2,\cdots,N_2 \tag{1}$$

where $R_q^{U_i}(q=1,2,\cdots,n)$ is the quantity of the qth type of resources of U_i.

Let $T=\{T_1,T_2,\cdots,T_M\}$ be the set of M stationary targets, and the information of targets is unknown to UAV swarm at the initial time. m types of resources are required to destroy the jth target T_j, which are expressed as

$$\boldsymbol{R}^{T_j}=(R_1^{T_j},R_2^{T_j},\cdots,R_m^{T_j}),\quad j=1,2,\cdots,M \tag{2}$$

where $R_p^{T_j}(p=1,2,\cdots,m)$ is the quantity of the pth type of resources required for T_j. Assuming the type of re-

sources carried by UAVs is the same as that required by the targets, that is, $m = n$.

The basic process of UAV swarm cooperatively search-attack can be divided as two stages of search and attack, as shown in Fig. 1. At the search stage, UAV swarm performs collaborative search task in the unknown environment. When T_j is detected by U_i, the position (x^{T_j}, y^{T_j}), value V^{T_j}, and resource requirement $\boldsymbol{R}^{T_j}$ of T_j can be obtained by the UAV swarm, and then the UAV swarm turns to the attack stage. At the attack stage, the attacking task of T_j is assigned to RS-UAVs according to the states of T_j and UAVs.

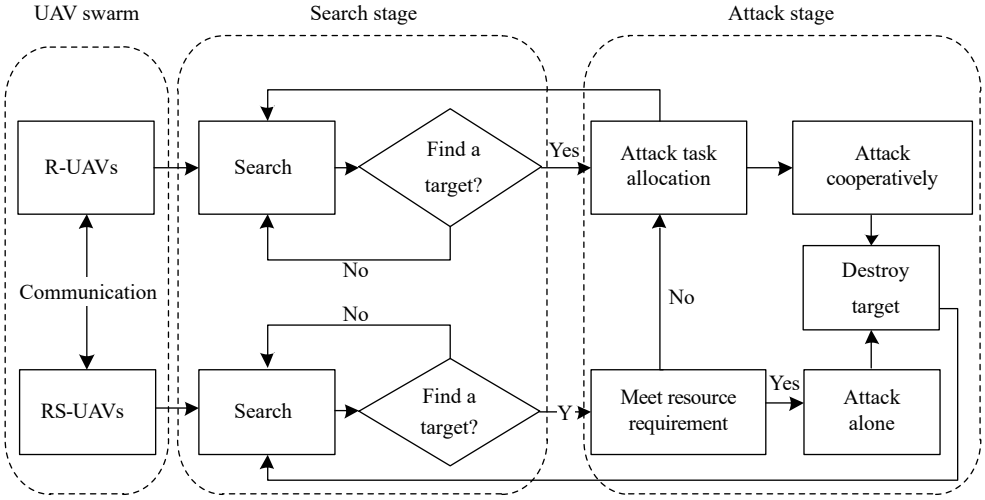

Fig. 1 Basic process of UAV swarm cooperative search-attack

If $R_p^{U_i} \geqslant R_p^{T_j}, \forall p = 1,2,\cdots,m$, U_i attacks T_j independently without assistance. Otherwise the attacking task of T_j is assigned and then an attacking coalition is formed using the task allocation algorithm. Because the task allocation operation mainly occurs in the attack stage, the optimization objective of the UAV swarm cooperative search-attack mission planning can be denoted by the maximum attack efficiency of RS-UAVs. The attack efficiency J is composed of attack reward (target value) and attack cost (path length cost and time cost).

$$J = \max \sum_{j=1}^{M} \left(\omega_1 \cdot V^{T_j} - \omega_2 \cdot \sum_{i=1}^{n_c^j} (\bar{d}_{ij} + \bar{t}_{ij}) \right)$$

s.t.

$$\begin{cases} \sum_{i=1}^{n_c^j} R_p^{U_i} \geqslant R_p^{T_j}, \quad p = 1,2,\cdots,m \\ G(x) \leqslant 0 \end{cases} \tag{3}$$

where n_c^j is the number of UAVs participating in attacking T_j. $\bar{d}_{ij}$ and $\bar{t}_{ij}$ are the distance and time of U_i flying to T_j after normalization, respectively. ω_1 and ω_2 are the weights of attack reward and cost in the objective function, respectively.

The resource constraint in (3) indicates that the total resources of RS-UAVs in the attacking coalition should satisfy the resource requirements of T_j. The constraint $G(x)$ consists of the mobility constraint, the flying distance constraint of UAVs, etc.

3. Wolf scouting behavior-inspired cooperative covering search algorithm

3.1 Analysis of wolf scouting behavior

At the beginning of cooperative hunting, several scout wolves who have shrewd perception capability are sent to the hunting territory to search the prey widely [25,26,28]. The scouting behavior of scout wolves is simple and efficient, which follows the following three rules:

(i) Scout wolves can mark the searched area efficiently through the specific odor or trace using urine and feces.

(ii) As the search proceeds, the attraction level of the searched area decreases. By perceiving the legacy odor or trace, scout wolves can avoid the searched areas and further explore the unsearched areas.

(iii) Based on the real-time interaction between wolves, the local information obtained by different scout wolves can be integrated for the whole pack quickly.

3.2 Search environment model

Due to the simple implementation and strong expression ability, the grid-based method is adopted here to discretely model the search environment of scout wolves.

Assuming the search environment is a plane rectangular region, and the rectangular region is divided into $L_x \times L_y$ discrete grids, as shown in Fig. 2. $\text{Grid}_{(m,n)}$ denotes the grid at the mth row and the nth column, then the search environment E of scout wolves can be represented by the set of grids as

$$E = \{\text{Grid}_{(m,n)} | m = 1, 2, \cdots, L_y, n = 1, 2, \cdots, L_x\}. \quad (4)$$

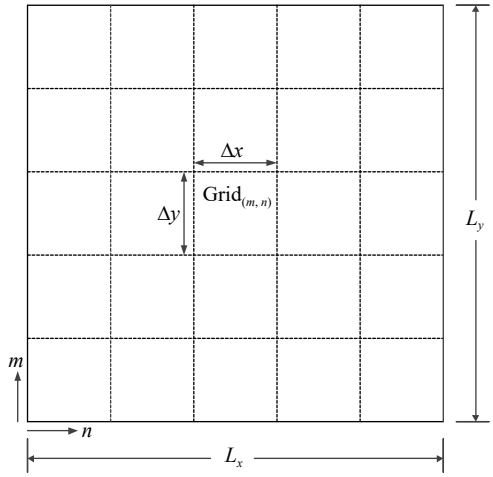

Fig. 2 Grided search environment of scout wolves

In Fig. 2, Δx and Δy are the length and width of a single square grid, respectively, which can be represented as the flight distance of UAVs in a time step at an average speed. At time t, the state of $\text{Grid}_{(m,n)}$ can be expressed as

$$\boldsymbol{state}_{(m,n)}(t) = [\boldsymbol{\mu}_{(m,n)}, \zeta_{(m,n)}, \eta_{(m,n)}(t)] \quad (5)$$

where $\boldsymbol{\mu}_{(m,n)}$ is the center point coordinate of $\text{Grid}_{(m,n)}$. $\zeta_{(m,n)} \in \{0, 1\}$ is the target existence status of $\text{Grid}_{(m,n)}$, $\zeta_{(m,n)} = 1$ indicates that there exists a target in $\text{Grid}_{(m,n)}$, and $\zeta_{(m,n)} = 0$ indicates that there exists no target in $\text{Grid}_{(m,n)}$. $\eta_{(m,n)}(t) \in \{0, 1, 2, \cdots, h\}$ is the times that $\text{Grid}_{(m,n)}$ has been searched by UAVs.

3.3 UAV movement model

By taking a UAV as a particle moving in the two-dimensional plane, UAVs can move from the center point of its current grid to the center point of the neighbored grid under the mobility constraint and search the grids within its detection range in each time step.

Let $\boldsymbol{state}_i(t)$ be the state of U_i at time t, which is expressed as

$$\boldsymbol{state}_i(t) = [\boldsymbol{\lambda}_i(t), o_i(t)] \quad (6)$$

where $\boldsymbol{\lambda}_i(t) = (x_i(t), y_i(t)) \Rightarrow (m_i(t), n_i(t))$ is the discrete position coordinate of U_i in E at time t, and the grid index of this coordinate is $(m_i(t), n_i(t))$. $o_i(t)$ and $\Delta o_i(t)$ are the course angle and yaw angle of U_i at time t, respectively.

The movement model of U_i can be given as

$$\begin{cases} x_i(t+1) = x_i(t) + \text{INT}[\bar{v} \cdot \Delta t \cdot \cos(o_i(t+1))/\Delta x] \\ y_i(t+1) = y_i(t) + \text{INT}[\bar{v} \cdot \Delta t \cdot \sin(o_i(t+1))/\Delta y] \\ o_i(t+1) = o_i(t) + \Delta o_i(t) \end{cases} \quad (7)$$

where $\Delta o_i(t) \in [-\Delta o_{\max}, \Delta o_{\max}]$, $\Delta o_{\max}$ is the maximum turning angle of UAVs, and $\bar{v}$ is the average speed of U_i. $\text{INT}[\cdot]$ is a rounding operator which aims at mapping the flight distance of UAVs into grid index increment $(\Delta m, \Delta n)$ in the grided search region.

In the grided search environment, $o_i(t)$ can be denoted as $o_i(t) \in \{0, 1, 2, 3, 4, 5, 6, 7\}$ with quantization operation as Fig. 3. Assuming $\Delta o_{\max} = 45°$, and then the relationship between the current course angle and the next optional course angle of UAVs under the UAV mobility constraint can be defined as

$$o_i(t+1) \in \{o_i(t) - 1, o_i(t), o_i(t) + 1\} \bmod 8 \quad (8)$$

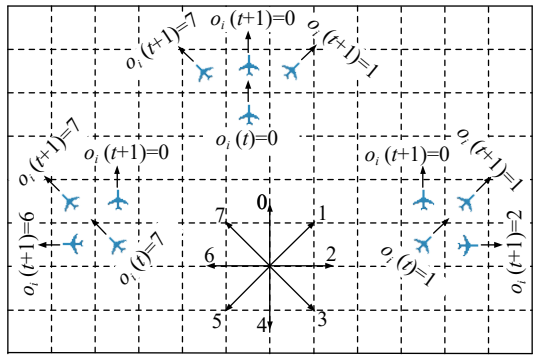

Fig. 3 Relationship between the current course angle and the next optional course angle of UAVs

3.4 UAV search strategy based on stimulus updating

To quantify UAVs' perception of the dynamic search environment information, a search stimulus $c_{(m,n)}$ is designed for each grid. The value of $c_{(m,n)}$ represents the search attractive level of $\text{Grid}_{(m,n)}$ for UAVs. As the search proceeds, the value of $c_{(m,n)}$ is constantly updated by

$$c_{(m,n)}(t) = c_{(m,n)}(0) \cdot \alpha^{\eta_{(m,n)}(t)} \quad (9)$$

where $c_{(m,n)}(0)$ is the initial search stimulus of $\text{Grid}_{(m,n)}$, and $\eta_{(m,n)}(t)$ is defined as (5). $\alpha \in (0, 1)$ is the stimulus attenuation coefficient.

As for U_i, U_i will select the grid with the largest search stimulus as its next search point at time t, then

$$(m_i^*(t+1), n_i^*(t+1)) = \arg \max_{\{m_i(t), n_i(t)\}} c_{(m_i(t), n_i(t))} \quad (10)$$

where $(m_i^*(t+1), n_i^*(t+1))$ is the grid index of the next search point selected by U_i.

According to (9), the search stimuli of the searched grids gradually decrease, and the more times the grids are searched, the smaller the value of their search stimuli. Under the action of (10), UAVs always tend to move towards the grids with relatively large search stimuli, and the unsearched area can be explored and the repeated

search can be avoided effectively. In this way, the high search covering rate and search efficiency can be guaranteed. Moreover, the searching decision strategy of UAVs presented in (9) and (10) have the characteristics of simple calculation and easy implementation, which helps to improve the search speed of UAV in uncertain environment. The search decision process of UAVs is shown as Fig. 4.

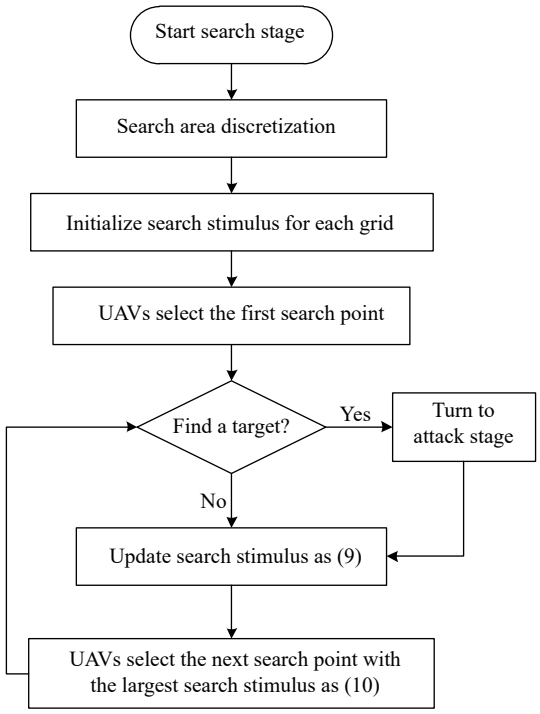

Fig. 4 Search decision process of UAVs

To facilitate the study, we make the following assumptions.

(i) There is at most one target in each grid.

(ii) UAVs have the autonomous obstacle avoidance ability, so the obstacles in the task environment are not considered.

(iii) Each UAV can communicate with each other without considering the communication delay.

4. Wolf pack labor division behavior-based task allocation algorithm

4.1 Analysis of wolf pack's role-task matching labor division mechanism

Labor division behavior refers to different individuals performing different tasks. It is distributed throughout the social biological groups. Labor division is an important swarm intelligence behavior, which is instructive to solve complex multi-task allocation problems with high efficiency in dynamic environments [29,30].

Wolves have role differentiations in cooperative hunting, that is, individuals with different roles perform specific subtasks that match their roles [26,27]. The basic mechanism of labor division in wolf pack is a role matching task. An intelligent and experienced individual acts as the leader wolf to command the group action, the perceptive individuals act as the scout wolves to search for prey, the swift individuals act as the fierce wolves to harass the prey group, and the strong and aggressive individuals act as the giant wolves to besiege the single prey [31,32].

Moreover, wolves can switch their roles flexibly to meet the changing task requirements [33]. For example, if giant wolves cannot kill the prey, several scout wolves and fierce wolves convert to giant wolves immediately to assist to complete the besieging task. Through the flexible transformation and dynamic reorganization of individual roles, the subtasks of command, search, harass, and besieging can be allocated and performed with high efficiency.

In essence, the role-task matching labor division is an oriented task allocation, and the flexible role transformation and task adjustment of wolf pack can be seen as the dynamic task re-allocation.

4.2 Wolf pack labor division model (WPLDM)

Based on the role-task matching mechanism, the WPLDM is built as Fig. 5.

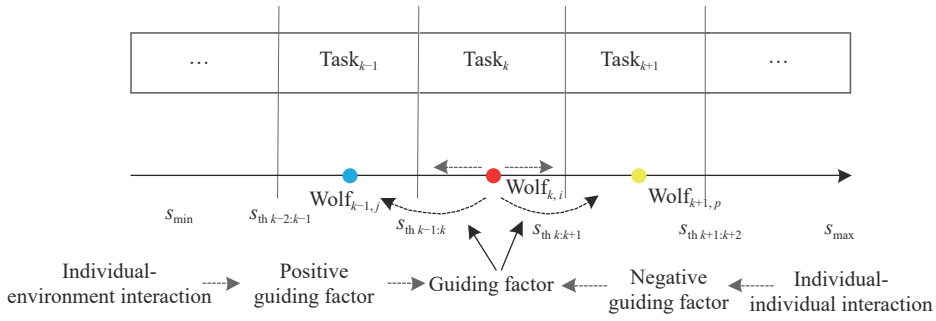

Fig. 5 WPLDM

Let $\text{Task}=\{\text{Task}_1,\text{Task}_2,\cdots,\text{Task}_m\}$ be the set of m tasks, and $\text{Task}_k(k=1,2,\cdots,m)$ is the kth subtask. The wolf pack composed of m different types of roles is represented as $\text{Wolf}=\{\text{Wolf}_1,\text{Wolf}_2,\cdots,\text{Wolf}_m\}$, and Wolf_k $(k=1,2,\cdots,m)$ is the set of wolves with the kth type of roles. Wolf_k matches and performs the kth subtask. Let $\text{Wolf}_{k,i}$ be the ith wolf in Wolf_k and $s_{k,i}\in(s_{\text{th}\,k-1:k},s_{\text{th}\,k:k+1})$ be the role state variable of $\text{Wolf}_{k,i}$.

To respond to the change of task requirement, wolves need to shift their roles by adjusting their role state variables. The adjustment of the role state variable $s_{k,i}$ of $\text{Wolf}_{k,i}$ can be expressed as

$$s_{k,i}(t+1)=f(s_{k,i}(t),\delta_{k,i}(t)) \tag{11}$$

where $\delta_{k,i}$ is the guiding factor which denotes the guiding effect of tasks on $s_{k,i}$ at time t.

The guiding factor δ reflects the comprehensive results of individual-individual interaction and individual-environment interaction. Let δ^+ be the positive guiding factor to measure the individual-environment interaction and δ^- be the negative guiding factor to measure the individual-individual interaction of wolves, respectively. Then δ can be obtained by $\delta=\delta^+/\delta^-$, and the maximum guiding effect on $s_{k,i}$ can be expressed as

$$\tilde{\delta}_{k,i}^{k^*}=\arg\ \max\ (\delta_{k,i}^{+}/\delta_{k,i}^{-}) \tag{12}$$

where k^* is the sequence number of the task that has the greatest guiding effect on $s_{k,i}$.

The role state variable $s_{k,i}$ of $\text{Wolf}_{k,i}$ is updated by

$$s_{k,i}(t+1)=\begin{cases} s_{k,i}(t)+\tau\cdot\exp\tanh\left(\tilde{\delta}_{k,i}^{k^*}\right), & \tilde{\delta}_{k,i}^{k^*}>l_u;k^*>k \\ s_{k,i}(t)-\tau\cdot\exp\tanh\left(\tilde{\delta}_{k,i}^{k^*}\right), & \tilde{\delta}_{k,i}^{k^*}>l_u;k^*<k \\ s_{k,i}(t)+\tau\cdot\text{rand}(-1,1), & \text{otherwise} \end{cases} \tag{13}$$

where k is the sequence number of the task currently executed by $\text{Wolf}_{k,i}$, τ and l_u are step adjustment coefficient and role adjust threshold, respectively.

According to (13), if $\tilde{\delta}_{k,i}^{k^*}$ exceeds l_u and k^* is greater than k, $s_{k,i}$ increases. If $\tilde{\delta}_{k,i}^{k^*}$ exceeds l_u and k^* is smaller than k, $s_{k,i}$ decreases. Otherwise $s_{k,i}$ moves in random to prevent deadlock. The greater the $\tilde{\delta}_{k,i}^{k^*}$, the faster the role transition.

Based on the role-task matching mechanism, $\text{Wolf}_{k,i}$ transforms its role according the updated $s_{k,i}$ and then it performs the new task that matches the updated role.

$$\text{new\_Task}=\begin{cases} \text{Task}_{k+1}, & s_{\text{th}\,k+1:k+2}>s_{k,i}>s_{\text{th}\,k:k+1} \\ \text{Task}_{k-1}, & s_{\text{th}\,k-2:k-1}>s_{k,i}>s_{\text{th}\,k-1:k} \\ \text{Task}_k, & \text{otherwise} \end{cases} \tag{14}$$

As can be seen from (14), when $s_{k,i}$ updates and moves to the interval of $(s_{\text{th}k:k+1},s_{\text{th}k+1:k+2})$, the role of $\text{Wolf}_{k,i}$ converts to Wolf_{k+1}, and then $\text{Wolf}_{k,i}$ chooses and executes Task_{k+1}. When the updated $s_{k,i}$ moves to the interval of $(s_{\text{th}k-2:k-1},s_{\text{th}k-1:k})$, the role of $\text{Wolf}_{k,i}$ converts to Wolf_{k-1}, and then $\text{Wolf}_{k,i}$ executes Task_{k-1}. When the updated $s_{k,i}$ remains in the interval of $(s_{\text{th}k-1:k},s_{\text{th}k:k+1})$, the role of $\text{Wolf}_{k,i}$ remains unchanged, and then $\text{Wolf}_{k,i}$ executes its previously assigned Task_k.

4.3 Task allocation strategy based on WPLDM

The division labor model constructed in Subection 4.2 is a general multi-task allocation approach, while the task allocation for the discovered T_j only involves a single target and a single attack task. The attack task execution state of U_i can be expressed as

$$\theta_{(i,j)}=\{0,1\},\ i=1,2,\cdots,N_2;j=1,2,\cdots,M \tag{15}$$

where $\theta_{(i,j)}=1$ indicates that U_i attacks T_j, $\theta_{(i,j)}=0$ indicates that U_i does not attack T_j.

As for the UAV swarm cooperative attack task allocation problem when T_j has been searched, the positive guiding factor $\delta_{i,j}^{+}$ can be transformed as

$$\delta_{i,j}^{+}=\frac{V^{T_j}}{\omega_1\cdot\bar{d}_{ij}+\omega_2\cdot\bar{t}_{ij}} \tag{16}$$

where V^{T_j} is the value of T_j. $\bar{d}_{ij}$ and $\bar{t}_{ij}$ are the normalized distance cost and time cost of U_i flying to T_j under mobility restrictions, respectively. ω_1 and ω_2 are weight coefficients and $\omega_1+\omega_2=1$.

In (16), $\delta_{i,j}^{+}$ reflects the interaction result between U_i and T_j, which can be seen as the attractive effect of U_i performing T_j.

Similarly, the negative guiding factor $\delta_{i,j}^{-}$ can be transformed as

$$\delta_{i,j}^{-}=\frac{n_c^j}{1-\partial^j} \tag{17}$$

where ∂^j is the completion degree of T_j as defined in (18). n_c^j is the number of UAVs participating in attacking T_j.

In (17), $\delta_{i,j}^{-}$ reflects the interaction result between UAVs, which can be seen as the repulsive effect of U_i performing T_j.

$$\partial^j(t)=\frac{\sum_{p=1}^{m}R_p^{T_j}(t)}{\sum_{p=1}^{m}R_p^{T_j}(0)} \tag{18}$$

where $R_p^{T_j}(0)$ and $R_p^{T_j}(t)$ are the resource requirements of T_j at the initial time and time t, respectively.

Let $s_{i,j}$ be the role state variable of U_i. Assume that the attack task execution state of U_i is $\theta_{(i,j)}=0$ at time t, then the role transformation and task adjustment of U_i in the next time step is shown as Fig. 6.

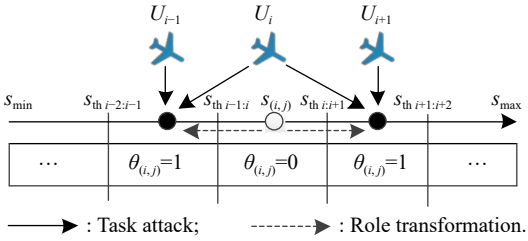

Fig. 6 Role transformation and task adjustment of U_i

In Fig. 6, the value of $\theta_{(i,j)}$ switches from 0 to 1 by the role transformation of U_i, and then U_i is selected to attack T_j. The role transformation and task adjustment of U_i are realized by (19) and (20), respectively.

$$s_{i,j}(t+1)=\begin{cases} s_{i,j}(t)\pm\tau\cdot\exp\tanh(\delta_{i,j}), & \delta_{i,j}>l_u \\ s_{i,j}(t)+\tau\cdot\text{rand}(-1,1), & \text{otherwise} \end{cases} \tag{19}$$

$$\theta_{(i,j)}=\begin{cases} 1, & s_{i,j}\in(s_{\text{th }i:i+1},s_{\text{th }i+1,i+2})\,\text{or}\,(s_{\text{th }i-2:i-1},s_{\text{th }i-1:i}) \\ 0, & \text{otherwise} \end{cases} \tag{20}$$

From the perspective of theoretical analysis, the proposed WPLDM-based task allocation method has the following two potential advantages:

(i) Balance between solution quality and solving speed. Conventional intelligent optimization algorithms, such as particle swarm optimization (PSO), ant colony optimization (ACO) and genetic algorithm (GA), all have a contradiction between algorithm speed and accuracy and often need to sacrifice the computational speed to obtain the optimal solution [34,35]. Moreover, these algorithms need to evaluate all feasible solutions to obtain the optimal solution with large computation cost.

The proposed task allocation algorithm is based on the stimulus-response mode, which simulates the individuals' quick response to the task and environment through local perception and interaction. UAVs only need to make decisions according to its own state, friendly UAVs states, and the task state, and the task allocation calculation is very simple, which results in the good real-time performance and high solving efficiency. Furthermore, through the comprehensive consideration of task value, resource requirement of tasks, remaining resources of UAVs, task completion degree and the number of UAVs performing the task as shown in (16)−(18), the task allocation solution has good operability and rationality. In this way, the proposed algorithm can obtain a high quality task allocation scheme with fast speed.

In practice, the core of the UAV swarm search-attack mission planning in uncertain battle environment is to properly allocate the appropriate tasks to the appropriate UAVs in real-time. Therefore, the proposed algorithm has good practicability due to its good balance between solving speed and solution quality.

(ii) Robustness and scalability. The efficiency of the conventional intelligent optimization algorithm is highly related to the diversity and size of the population [36], while it is difficult to maintain the population diversity in the iterations. If the population size is small or the population distribution is not evenly enough in the search space, the solution quality cannot be guaranteed. Due to the centralized solving architecture, the robustness and scalability performance of these algorithms are dissatisfactory.

The proposed task allocation algorithm is based on the distributed solving architecture, each UAV is designed as an agent with a certain degree of independent decision-making ability. Moreover, the design idea of the algorithm originates from the flexible transformation of wolves' roles according to the characteristics of the task and the adaptive adjustment of the group task of wolf pack, the algorithm is very similar to biological characteristics and interpretable. Therefore, the change of the number of tasks and UAVs has little effect on the performance of the algorithm, which reflects the good robustness and scalability of the proposed algorithm.

4.4 Basic processes of wolf hunting behavior-based mission planning algorithm for UAV swarm cooperative search-attack

Based on the previous analyses, the mapping relationship between wolf pack hunting behavior and UAV swarm cooperative search-attack can be constructed as Table 1.

Table 1 Mapping relationship between wolf pack hunting and UAV swarm cooperative search-attack

Behavior characteristics	Wolf pack hunting	UAV swarm cooperative search-attack
Behavior actor	Wolf pack	UAV swarm
	Prey	Target
Behavior space	Hunting territory	Task environment
	Scouting	Search target
Specific behavior	Labor division	Attack task allocation
	Besieging	Coordinated attack

As can be seen from Table 1, the corresponding mapping relationship can be described as follows:

(i) Each UAV is equivalent to a wolf;

(ii) The prey is regarded as the target;

(iii) The scouting behavior of wolves can be seen as the search stage of UAVs;

(iv) The labor division of wolves in cooperatively

hunting is modeled as the attack task allocation among RS-UAVs;

(v) The role transformation and task adjustment among wolves is regarded as the flexible attack task re-allocation.

The basic processes of wolf hunting behavior-based mission planning algorithm for UAV swarm cooperative search-attack are shown in Fig. 7 and corresponding descriptions are shown as follows.

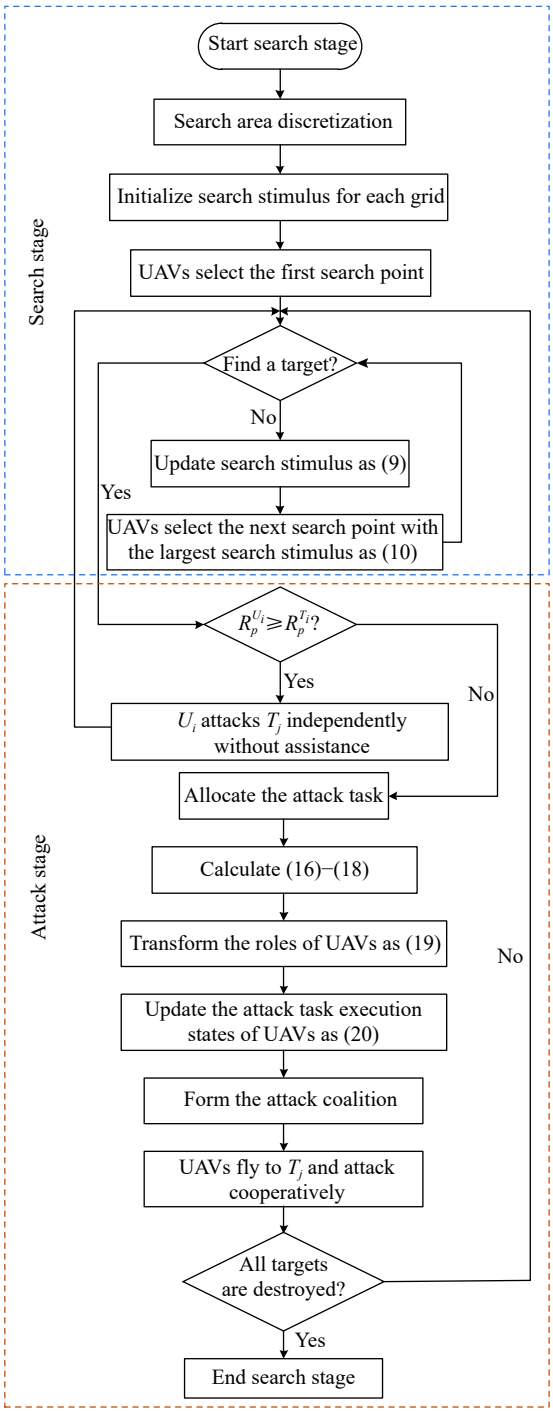

Fig. 7 Basic processes of wolf hunting behavior-based mission planning algorithm for UAV swarm cooperative search-attack

Step 1 UAV swarm searches tasks in unknown environment based on the wolf scouting behavior-inspired cooperative covering search algorithm as defined in Section 3.

Step 2 Compare the resource requirement $\boldsymbol{R}^{T_j}$ of T_j and the available resources $\boldsymbol{R}^{U_i}$ of U_i when T_j is searched by U_i.

Step 3 If $R_p^{U_i} \geqslant R_p^{T_j}, \forall p = 1, 2, \cdots, m$, U_i attacks T_j independently without assistance. Otherwise the attack task of T_j is assigned using the wolf pack labor division behavior-based task allocation algorithm as Section 4.

Step 4 UAVs assign the attack task flying to T_j and perform the attack task cooperatively. UAVs that do not perform the attack task continue to search the unexplored environment.

Step 5 If a new target is searched, turn to Step 2. If all targets have been discovered and destroyed, turn to termination.

5. Simulation experiments and results analyses

The performances of the proposed algorithm for UAV swarm cooperative search-attack mission planning are verified by three groups of independent experiments. In the first group experiment, the effectiveness and feasibility of the proposed algorithm are tested using six heterogeneous UAVs to search and attack three unknown targets. Based on the Monte-Carlo method, the influence of UAVs and targets number on the proposed algorithm is analyzed in the second group experiment, and its stability and scalability are evaluated as well. The performance of the proposed wolf scouting behavior-inspired search algorithm is tested in the third group experiment. All simulation experiments are conducted on Matlab 2017b.

5.1 Effectiveness and feasibility experiment

The UAV swarm, composed of two R-UAVs and four RS-UAVs, aims to search and attack three unknown targets. Corresponding parameters of UAVs and targets are shown in Table 2 and Table 3, respectively. The combat environment is a 2 000 m×2 000 m plan region which is divided into 50×50 discrete square grids. The detection radius of RS-UAVs is 60 m, that is, R-UAVs can search nine grids centered on their current grids for a certain time step. The detection radius of R-UAVs is 20 m, and R-UAVs can only search its located grid. Each UAV moves with the speed as defined in Section 3.

The parameters of the proposed algorithm in the experiment are set as follows: the initial search stimulus $c_{(m,n)}(0) = 100$, stimulus attenuation coefficient $\alpha = 0.1$, step adjustment coefficient $\tau = 0.5$, and role adjust threshold l_u=0.8, $s_{\min}$=1, $s_{\max}$=10, ω_1=0.5 and ω_2=0.5.

Table 2 Parameters of heterogeneous UAVs

UAV (U_i)	Type	Initial resource	Initial position (x_i, y_i)/m	Initial course angle o_i/(°)
U_1	RS-UAV	(1,2,1)	(180,20)	45
U_2		(2,1,0)	(500,20)	90
U_3		(2,2,1)	(820,20)	135
U_4		(1,1,3)	(1 180,20)	45
U_5	R-UAV	(0,0,0)	(1 500,20)	90
U_6		(0,0,0)	(1 820,20)	135

Table 3 Parameters of targets

Target (T_j)	Initial resource requirement	Position(x_j, y_j)/m	Value
T_1	(3,2,1)	(780,780)	3
T_2	(2,3,1)	(1 620,980)	5
T_3	(1,0,2)	(980,1 620)	4

The complete operation process of six heterogeneous UAVs cooperatively searching and attacking three targets is shown as Fig. 8. At the beginning, UAVs start from their initial positions to search the unknown targets based on the wolf scouting behavior-inspired search algorithm, separately.

The initial states of UAVs and targets are shown as Fig. 8(a). At t=16.9 s, T_2 is discovered by U_6 as shown in Fig. 6(b). Because U_6 is an R-UAV and its attack resource vector is (0,0,0), which means U_6 cannot perform the attack task of T_2. In this case, the task allocation operation is triggered, and then T_2 is assigned to U_3 and U_4 quickly based on the proposed wolf pack labor division-based task allocation algorithm. U_3 and U_4 arrive at T_2 at t=18.2 s and t=19.4 s respectively to cooperatively attack T_2 as Fig. 8(c).

As shown in Fig. 8(d), T_1 is discovered by U_1 at t= 19.2 s. Since the available resources (1,2,1) of U_1 cannot satisfy the resource requirement (3,2,1) of T_1, the attack task of T_1 is assigned to U_2 simultaneously. U_2 arrives at T_1 at t=21.4 s to assist U_1 to destroy T_1 as Fig. 5(e). At t=25.7 s, T_3 is discovered by U_6 as Fig. 8(f), and U_4 is assigned to attack T_3 as shown in Fig. 8(g). The remaining resources (1,0,3) of U_4 meet the resource requirement (1,0,2) of T_3, that is, U_4 can destroy T_3 without assistance. Overall, the complete search and attack process of UAVs is very compact. Once a target is found, it can be quickly attacked and destroyed. The total time for UAV swarm to complete all targets is 28.8 s, which reflects that the proposed search and attack task allocation algorithms have good real-time performance.

To further analyze the effectiveness of the task allocation results, the resource requirements of targets and the available resources of RS-UAVs in different time points are presented in Table 4.

In Table 4, the time points when the targets are attacked by RS-UAVs are presented in the first column, and the resource requirements of targets and the available resources of RS-UAVs at each attacking time point can be seen from the third and fourth columns, respectively. From Table 4, it can be concluded that the total resources of RS-UAVs can well meet the resource requirements of their assigned target, which means that the targets can be destroyed successfully and the task allocation results are effective.

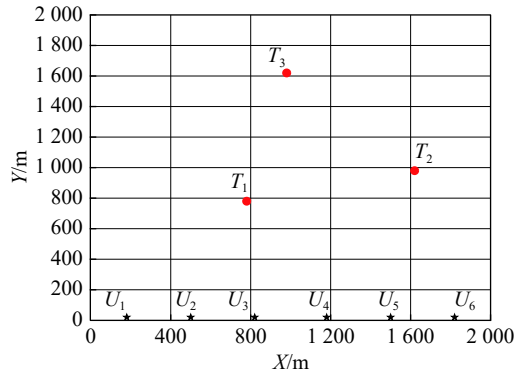

(a) Initial states of UAVs and targets

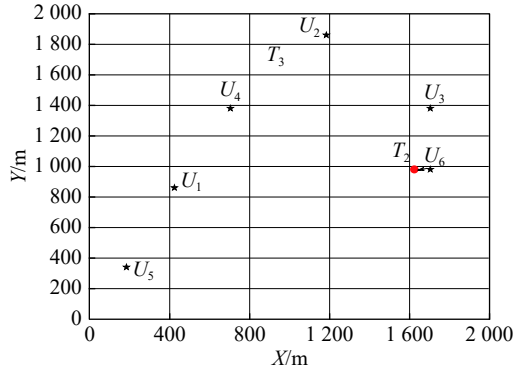

(b) T_2 discovered by U_6 at 16.9 s

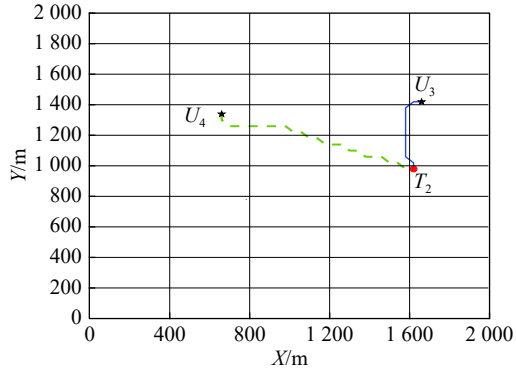

(c) U_3 (arriving at 18.2 s) and U_4 (arriving at 19.4 s) attacking T_2 cooperatively

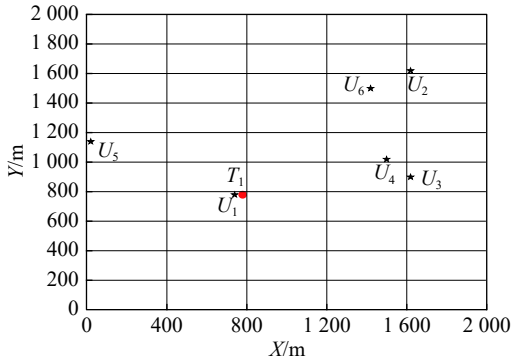

(d) T_1 discovered by U_1 at 19.2 s

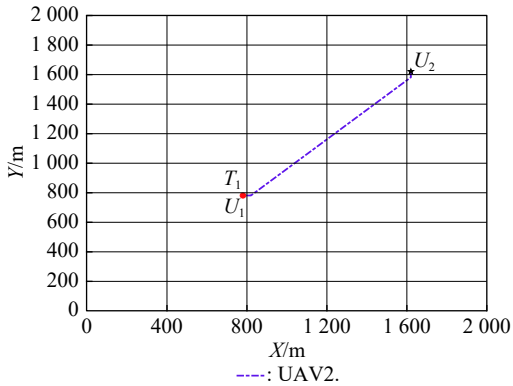

(e) U_1 (arriving at 19.2 s) and U_2 (arriving at 21.4 s) attacking T_1 cooperatively

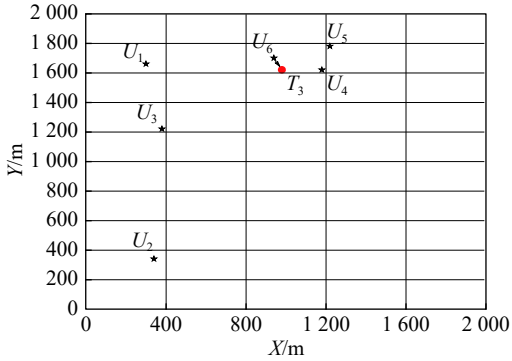

(f) T_3 discovered by U_6 at 25.7 s

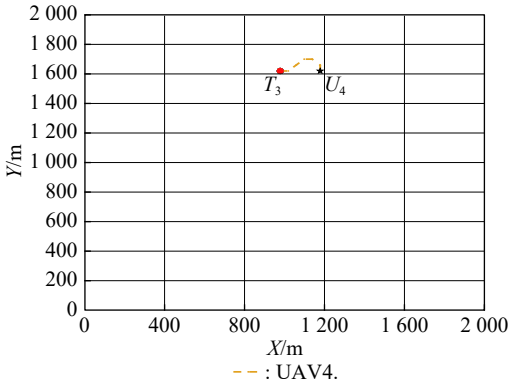

(g) U_4 (arriving at 28.8 s) attacking T_3 without assistance

Fig. 8 Complete operation process of six UAVs cooperative searching and attacking three targets

Table 4 Resource requirements of targets and UAV resources in different time points

Time/s	Target	Target resource requirement	UAV resource	Remaining resource
18.2	T_2	(2,3,1)	U_3(2,2,1)	(0,0,0)
19.4		(0,1,0)	U_4(1,1,3)	(1,0,3)
19.2	T_1	(3,2,1)	U_1(1,2,1)	(0,0,0)
21.4		(2,0,0)	U_2(2,1,0)	(0,1,0)
28.8	T_3	(1,0,2)	U_4(1,0,3)	(0,0,1)

5.2 Stability and scalability experiment

To evaluate the stability and scalability of the proposed algorithm under the effect of different numbers of UAVs and targets, 12 groups of independent experiments with 5, 10, 15, and 20 UAVs and 5, 10, and 15 targets are conducted for 50 times, respectively. The combination ratio between R-UAVs and RS-UAVs in the experiments are set as Table 5.

Table 5 Combination ratio between R-UAVs and RS-UAVs

UAV swarm	Number of UAVs			
R-UAVs	1	2	3	4
RS-UAVs	4	8	12	16

For fairness concerning, the DACLD [22] and the hierarchical mission planning method (HMPM) [37] are selected as comparison algorithms. DACLD is an ant colony labor division-inspired task allocation algorithm, and HMPM is a contract network-based task allocation algorithm. Both DACLD and HMPM present outstanding performances for UAV swarm cooperative search-attack mission planning.

The average mission completion rate (AMCR) and the average mission completion time (AMCT) are computed as comparison indicators. AMCR is the average value of the ratio of the number of successfully destroyed targets to the total number of targets in a predetermined mission time range in 50 independent experiments. AMCT is the average time taken for destroying all targets in 50 independent experiments. The termination condition of the three algorithms is that all targets have been successfully searched and destroyed, or the operating time reaches the maximum mission time 300 s. The task environment and algorithm parameters are the same as Subsection 5.1.

The results of AMCRs of the three algorithms with different numbers of UAVs and targets are shown as Fig. 9. As can be seen from Fig. 9, when the numbers of targets are fixed, the AMCRs of the three algorithms rise with the increase of the numbers of UAVs. When the numbers of UAVs are fixed, the AMCRs of the three algorithms

decrease with the increase of the numbers of targets. It can be seen from Fig. 9(a) that the proposed algorithm can achieve 100% AMCR values with 15 and 20 UAVs when the number of targets is 5, while HMPM and DACLD need 20 UAVs to achieve 100% AMCR values. As can be seen from Fig. 9(b) and Fig. 9(c), when the number of targets is larger than 10, none of the three algorithms can achieve 100% AMCR values. In general, compared with HMPM and DACLD, the proposed algorithm can achieve the best AMCR results in all cases.

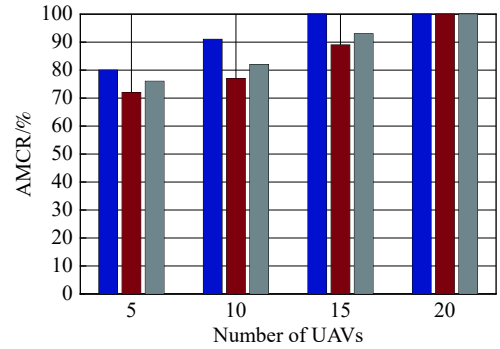

(a) AMCRs of the three algorithms with 5 targets

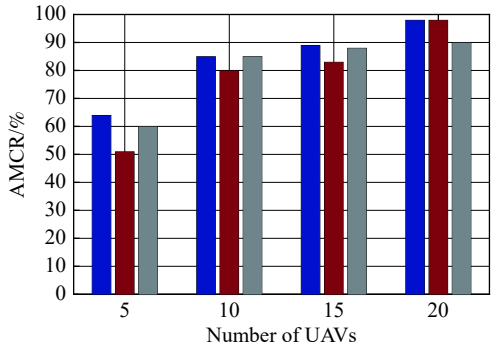

(b) AMCRs of the three algorithms with 10 targets

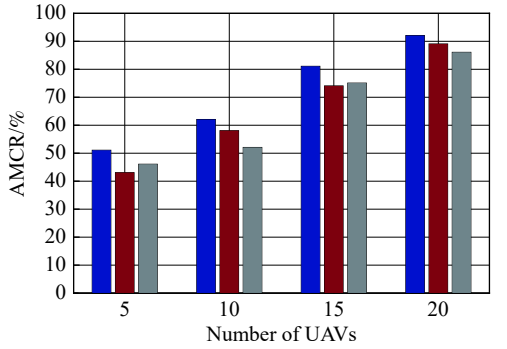

(c) AMCRs of the three algorithms with 15 targets

Fig. 9 AMCRs of the three algorithms with different numbers of UAVs and targets

The results of AMCTs of the three algorithms with different numbers of UAVs and targets are shown as Fig. 10.

As can be seen from Fig. 10, when the numbers of targets are fixed, the AMCTs of the three algorithms decrease with the increase of the numbers of UAVs. When the numbers of UAVs are fixed, the AMCTs of the three algorithms increase with the increase of the target number. In general, the proposed algorithm takes the shortest mission completion time among the three algorithms in all cases.

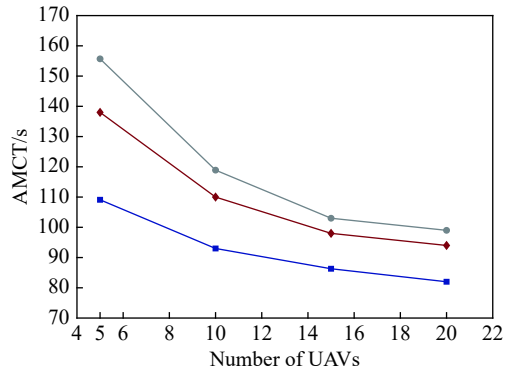

(a) AMCTs of the three algorithms with 5 targets

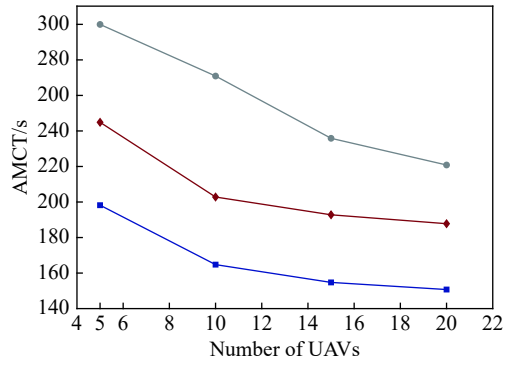

(b) AMCTs of the three algorithms with 10 targets

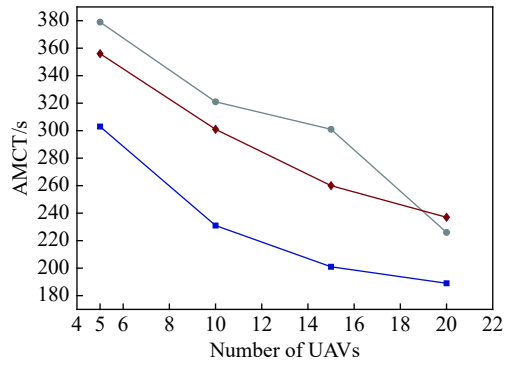

(c) AMCTs of the three algorithms with 15 targets

Fig. 10 AMCTs of the three algorithms with different numbers of UAVs and targets

In HMPM, the random search strategy is adopted in the UAV search stage, the phenomenon of repeated search is

serious and UAVs take a relatively long time to search for all targets, which results in the relatively long time for completing searching and attacking tasks. In DACLD, the task allocation strategy is based on the ant colony labor division model and UAVs perform tasks with the probability-based decision-making strategy, which results in that the algorithm takes a long time to find the most suitable RS-UAVs to attack a discovered target. In comparison, the proposed algorithm adopts the wolf hunting behavior-inspired search strategy in the UAV search stage, the repeated search can be avoided and the search efficiency can be developed effectively. Moreover, the target attack tasks are assigned to UAVs based on the simple interaction rules, and UAVs can make decisions quickly, which results in the good real-time performance of the proposed task allocation algorithm.

From Fig. 9 and Fig. 10, it can be concluded that the proposed algorithm performs better than the compared algorithms in terms of AMCR and AMCT. The effects of UAV and target number on the proposed algorithm are not significant, which shows that the proposed algorithm has superior stability and scalability.

5.3 Search performance experiment

To test the performance of the proposed wolf hunting behavior-inspired search algorithm, the search performance experiment is conducted by comparing with random search and the parallel search methods. The search environment is the same as Subsection 5.1, and the search time limitation is 300 s. In the comparison experiment, the numbers of UAVs are set as 5, 10, 15, and 20 and the average coverage rate (ACR) of the three search algorithms is compared. ACR is the average value of the rate of the number of searched grids to the total number of grids of 50 independent experiments, which is given by

$$\mathrm{ACR}=\frac{1}{50}\sum_{m=1}^{L_y}\sum_{n=1}^{L_x}\frac{\mathrm{Grid}_{(m,n)}}{L_x\times L_y},\quad \eta(m,n)\geqslant 1. \tag{21}$$

The curves of ACRs with the search time of the three search algorithms are presented in Fig. 11.

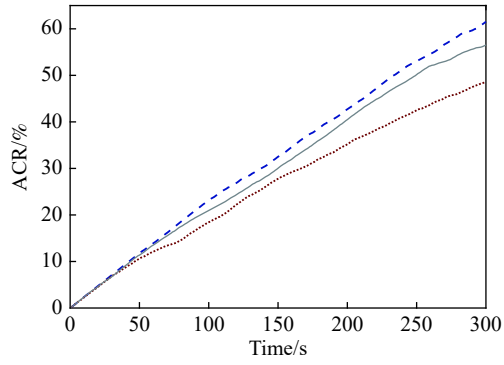

(a) 5 UAVs

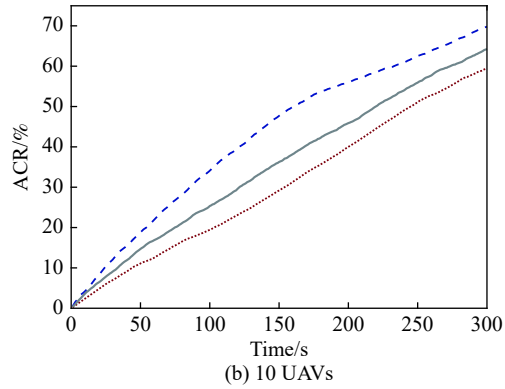

(b) 10 UAVs

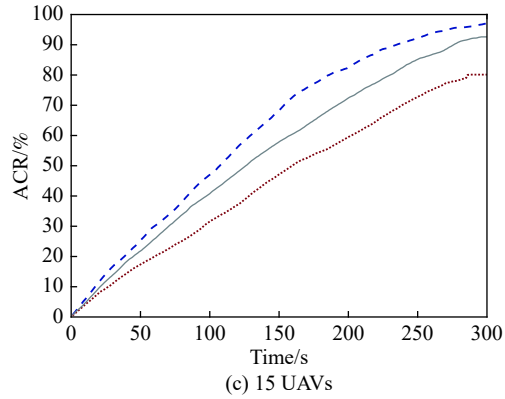

(c) 15 UAVs

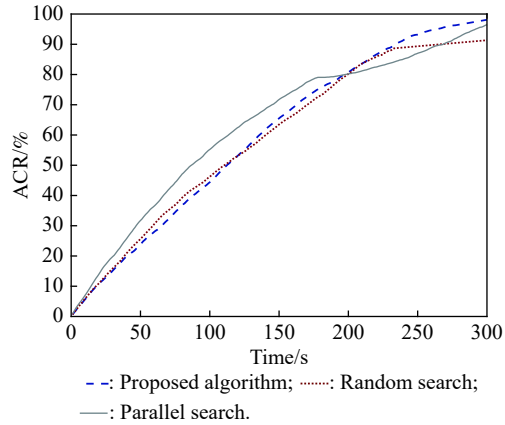

(d) 20 UAVs

Fig. 11 Curves of ACRs of the three search algorithms with different numbers of UAVs

As can be seen from Fig. 11, the ACRs of the three search algorithms rise as the search proceeds. In general, the proposed algorithm can obtain the largest ACR value, followed by parallel search, and then random search. It can be concluded that the proposed wolf hunting behavior-inspired search algorithm has competitive search efficiency and a high area covering level.

6. Conclusions

Inspired by the collaborative hunting behavior of wolf pack, a distributed and "bottom-up" self-organizing me-

thod for UAV swarm search-attack mission planning is proposed. In the search stage, UAVs can avoid repeated search efficiently using the wolf scouting behavior-inspired search algorithm. In the attack task allocation stage, UAVs can quickly assign the attack tasks by self-organizing using the proposed wolf pack labor division behavior-based task allocation algorithm.

The effectiveness, stability, and scalability of the proposed search and task allocation algorithms are verified by a set of simulation experiments. Our future research will focus on the in-depth theory analysis of the algorithm performance and the effect of parameter setting. Moreover, the algorithm performance for the large-scale UAV swarm in more complex and dynamic mission environment is also a promising research issue.

References

[1] HONG L, GUO H Z, LIU J J, et al. Toward swarm coordination: topology-aware inter-UAV routing optimization. IEEE Trans. on Vehicular Technology, 2020, 69(9): 10177–10187.

[2] WANG Y, RU Z Y, WANG K, et al. Joint deployment and task scheduling optimization for large-scale mobile users in multi-UAV-enabled mobile edge computing. IEEE Trans. on Cybernetics, 2020, 50(9): 3984–3997.

[3] KIM K S, KIM H Y, CHOI H L. A bid-based grouping method for communication-efficient decentralized multi-UAV task allocation. International Journal of Aeronautical and Space Sciences, 2020, 21(1): 290–302.

[4] ZHANG Y Z, FENG W C, SHI G Q, et al. UAV swarm mission planning in dynamic environment using consensus-based bundle algorithm. Sensors, 2020, 20(8): 2307–2327.

[5] ZHAO X Y, ZONG Q, TIAN B L, et al. Fast task allocation for heterogeneous unmanned aerial vehicles through reinforcement learning. Aerospace Science and Technology, 2019, 92: 588–594.

[6] XIE S Y, ZHANG A, BI W H, et al. Multi-UAV mission allocation under constraint. Applied Sciences, 2019, 9(11): 2184.

[7] MOON S, OH E, SHIM D H. An integral framework of task assignment and path planning for multiple unmanned aerial vehicles in dynamic environments. Journal of Intelligent & Robotic Systems, 2013, 70(1): 303–313.

[8] CHEN X, LIU Y T, YIN L Y, et al. Cooperative task assignment and track planning for multi-UAV attack mobile targets. Journal of Intelligent & Robotic Systems, 2020, 100(3): 1383–1400.

[9] HAFEZ A T, KAMEL M A. Cooperative task assignment and trajectory planning of unmanned systems via HFLC and PSO. Unmanned Systems, 2019, 7(2): 65–81.

[10] AUTENRIEB J, STRAWA N, SHIN H S, et al. A mission planning and task allocation framework for multi-UAV swarm coordination. Proc. of the Workshop on Research, Education and Development of Unmanned Aerial Systems, 2019: 297−304.

[11] SUN X L, QI N M, CHENG D, et al. Cooperative control algorithm of task assignment and path planning for multiple UAVs. Systems Engineering and Electronics, 2015, 37(12): 2772–2776. (in Chinese)

[12] MOUSAVI S, AFGHAH F, ASHDOWN J D, et al. Use of a quantum genetic algorithm for coalition formation in large-scale UAV networks. Ad Hoc Networks, 2019, 87: 26–36.

[13] YAN F L. Gauss interference ant colony algorithm-based optimization of UAV mission planning. The Journal of Supercomputing, 2020, 76(2): 1170–1179.

[14] ALHAQBANI A, KURDI H, YOUCEF-TOUMI K. Fish-inspired task allocation algorithm for multiple unmanned aerial vehicles in search and rescue missions. Remote Sensing, 2021, 13(1): 27–35.

[15] ZHEN Z Y, ZHU P, XUE Y X, et al. Distributed intelligent self-organized mission planning of multi-UAV for dynamic targets cooperative search-attack. Chinese Journal of Aeronautics, 2019, 32(12): 2706–2716.

[16] YAN F, ZHU X P, ZHOU Z, et al. Real-time task allocation for a heterogeneous multi-UAV simultaneous attack. Scientia Sinica Informationis, 2019, 49(5): 555–569. (in Chinese)

[17] ZHEN Z Y, XING D J, GAO C. Cooperative search-attack mission planning for multi-UAV based on intelligent self-organized algorithm. Aerospace Science & Technology, 2018, 76: 402–411.

[18] WU W N, CUI N G, GUO J F, et al. Distributed integrated method for mission planning of heterogeneous unmanned aerial vehicles. Journal of Jilin University (Engineering and Technology Edition), 2018, 48(6): 1827–1837. (in Chinese)

[19] YE F, CHEN J, SUN Q, et al. Decentralized task allocation for heterogeneous multi-UAV system with task coupling constraints. The Journal of Supercomputing, 2021, 77(1): 111–132.

[20] SLOWIK A, KWASNICKA H. Nature inspired methods and their industry applications —swarm intelligence algorithms. IEEE Trans. on Industrial Informatics, 2017, 14(3): 1004–1015.

[21] KIM M H, BAIK H, LEE S. Response threshold model based UAV search planning and task allocation. Journal of Intelligent & Robotic Systems, 2014, 75(3): 625–640.

[22] WU H S, LI H, XIAO R B, et al. Modeling and simulation of dynamic ant colony ’s labor division for task allocation of UAV swarm. Physica A: Statistical Mechanics & Its Applications, 2018, 491(2): 127–141.

[23] KURDI H, ALDAOOD M F, AL-MEGREN S, et al. Adaptive task allocation for multi-UAV systems based on bacteria foraging behaviour. Applied Soft Computing, 2019, 83: 105643.

[24] KURDI H A, EBTESAM A, MARAM A, et al. Autonomous task allocation for multi-UAV systems based on the locust elastic behavior. Applied Soft Computing, 2018, 71: 110–126.

[25] MURO C, ESCOBEDO R, SPECTOR L, et al. Wolf-pack (canis lupus) hunting strategies emerge from simple rules in computational simulations. Behavioural Processes, 2011, 88(3): 192–197.

[26] MECH L D. Alpha status, dominance, and division of labor in wolf packs. Canadian Journal of Zoology, 1999, 77(8): 1196–1203.

[27] MADDEN J D, ARKIN R C, MACNULTY D R. Multi-robot system based on model of wolf hunting behavior to emulate wolf and elk interactions. Proc. of the IEEE International Conference on Robotics & Biomimetics, 2011: 1043–1050.

[28] WU H S, XUE J J, XIAO R B, et al. Uncertain bilevel knapsack problem based on an improved binary wolf pack algorithm. Frontiers of Information Technology & Electronic Engineering, 2020, 21: 1356–1368.
[29] XIAO R B, WU H S, HU L, et al. A swarm intelligence labour division approach to solving complex area coverage problems of swarm robots. International Journal of Bio-Inspired Computation, 2020, 15(4): 224–238.
[30] XIAO R B, WANG Y C. Labour division in swarm intelligence for allocation problems: a survey. International Journal of Bio-Inspired Computation, 2018, 12(2): 8–12.
[31] LIANG W H, HE J H, WANG S X, et al. Improved cluster collaboration algorithm based on wolf pack behavior. Cluster Computing, 2019, 22(3): 6181–6196.
[32] BASSING S B, AUSBAND D E, MITCHELL M S, et al. Stable pack abundance and distribution in a harvested wolf population. The Journal of Wildlife Management, 2019, 83(3): 577–590.
[33] BUGLIONE M, TROISI S R, PETRELLI S, et al. The first report on the ecology and distribution of the wolf population in cilento, vallo di siano and alburni national park. Biology Bulletin, 2020, 47(6): 640–654.
[34] HU J Q, WU H S, ZHONG B, et al. Swarm intelligence-based optimisation algorithms: an overview and future research issues. International Journal of Automation and Control, 2020, 14(5/6): 656–693.
[35] PIOTROWSKI A P, NAPIORKOWSKI M J, NAPIORKOWSKI J J, et al. Swarm intelligence and evolutionary algorithms: performance versus speed. Information Sciences, 2017, 384: 34–85.
[36] NEDJAH N, MOURELLE L D M, MORAIS R G. Inspiration-wise swarm intelligence meta-heuristics for continuous optimisation: a survey−part I. International Journal of Bio-Inspired Computation, 2020, 15(4): 207–223.
[37] YAN F, ZHU X P, ZHOU Z, et al. A hierarchical mission planning method for simultaneous arrival of multi-UAV coalition. Applied Sciences, 2019, 9(10): 1986–2004.

Biographies

HU Jinqiang was born in 1990. He received his M.S. degree in vehicle operation engineering from Chang'an University, Xi'an, China, in 2017. He is currently a Ph.D. candidate with the School of Equipment Support and Management, Armed Police Force Engineering University. His current research interests include UAV swarm cooperative mission planning, swarm intelligent labor division approach, and swarm intelligence-based optimization algorithms.
E-mail: hujinqiang002@163.com

WU Husheng was born in 1986. He received his Ph.D. degree from Air Force Engineering University in 2014. He is now an associate professor of the School of Equipment Management and Support, Armed Police Force Engineering University, Xi'an, China. He is now engaged in the study of wolf pack algorithm, anti-terrorist cluster operations, and intelligent equipment.
E-mail: wuhusheng0421@163.com

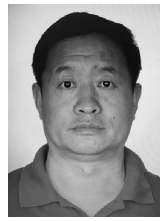

ZHAN Renjun was born in 1963. He is a full professor and Ph.D. supervisor at the School of Equipment Management and Support, Armed Police Force Engineering University, Xi'an, China. He received his Ph.D. degree from Xi'an Jiaotong University in 1996. He is a Senior Member of China Society of Mechanical Engineering. His current research interests are evolutionary computing, equipment support, and task allocation of UAV swarm.
E-mail: zhanrenjun@aliyun.com

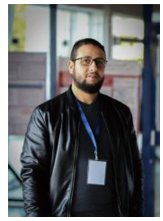

MENASSEL Rafik was born in 1983. He currently works at the Department of Mathematics and Computer Science, Tebessa University. He does research in computer graphics, artificial neural network, and artificial intelligence.
E-mail: r.menassel@univ-tebessa.dz

ZHOU Xuanwu was born in 1980. He is now a lecturer of Armed Police Command College. His current research interests are UAV swarm ad hoc network technology.
E-mail: schwoodchow@163.com